



**HAL**  
open science

## MOLECULAR DYNAMICS CALCULATIONS OF MICROCLUSTER PROPETES

W. Damgaard Kristensen, E. Jensen, R. Cotterill

► **To cite this version:**

W. Damgaard Kristensen, E. Jensen, R. Cotterill. MOLECULAR DYNAMICS CALCULATIONS OF MICROCLUSTER PROPETES. Journal de Physique Colloques, 1975, 36 (C2), pp.C2-21-C2-28. 10.1051/jphyscol:1975204 . jpa-00216251

**HAL Id: jpa-00216251**

**<https://hal.science/jpa-00216251>**

Submitted on 4 Feb 2008

**HAL** is a multi-disciplinary open access archive for the deposit and dissemination of scientific research documents, whether they are published or not. The documents may come from teaching and research institutions in France or abroad, or from public or private research centers.

L'archive ouverte pluridisciplinaire **HAL**, est destinée au dépôt et à la diffusion de documents scientifiques de niveau recherche, publiés ou non, émanant des établissements d'enseignement et de recherche français ou étrangers, des laboratoires publics ou privés.

## MOLECULAR DYNAMICS CALCULATIONS OF MICROCLUSTER PROPERTIES

W. DAMGAARD KRISTENSEN, E. J. JENSEN, R. M. J. COTTERILL

Department of Structural Properties of Materials, The Technical University of Denmark  
Building 307, DK-2800 Lyngby, Denmark

**Résumé.** — Les propriétés structurales et thermodynamiques des *microclusters* à 2 et 3 dimensions ont été étudiées par la technique de la dynamique moléculaire. Cette technique donne en principe pour chaque taille de cluster la configuration atomique de plus basse énergie libre. La fonction d'état des différents *microclusters* a été calculée en se servant d'une fonction de potentiel de paire de type Lennard-Jones tronquée.

On a étudié le processus de fusion ainsi que certaines propriétés telles que la température de fusion, la chaleur latente de fusion et les phénomènes de préfusion qui se sont révélés être dépendants de la taille du cluster aussi bien que de la structure de la phase solide.

**Abstract.** — The structural and thermodynamic properties of microclusters in two and three dimensions have been investigated by means of the molecular dynamics technique. This technique in principle produces the atomic configuration of lowest free energy for any given cluster size. The caloric equation of state for the different microclusters were calculated using a truncated Lennard-Jones pair potential. The nature of the melting transition was investigated and a number of properties, such as melting temperature, latent heat of melting, and premelting phenomena, were found to vary with cluster size, as well as with the structure of the solid phase.

**1. Introduction.** — Investigations of thermodynamic or structural properties of materials are usually concerned with the bulk behaviour, that is the properties that are measured in cases where surface effects are negligible. However, in extreme cases, the presence of a free surface can introduce dramatic deviations from the normal bulk behaviour. Heat capacity measurements on thin films in the neighbourhood of the bulk melting point [1], thus reveals that as the film gets thinner, the sharpness of the melting transition as well as the melting temperature decreases progressively. That also the structure of a material can be affected by a free surface is known from diffraction experiments on thin films and small particles. Electron diffraction experiments on a number of rare earth metals in the form of evaporated films [2] show that the bulk HCP structure is replaced by an FCC structure when the films are very thin. Electron diffraction studies of microclusters of argon atoms [3] formed by homogeneous nucleation show that the clusters are effectively of the bulk FCC structure, but contain vestiges of noncrystalline structure exhibited by the aggregates in the early stages of their growth. Numerous examples of the dependence of physical processes on the properties of very small atom clusters exist, including nucleation and growth, adsorption and catalysis, phase separation and precipitation, superconduction in thin films, processes in atmospheric physics, and the formation of glasses.

The first model which was applied to explain the properties of microclusters is based on the continuum

approximation [4]. It is assumed that the surface layer is infinitely thin and can be ascribed certain specific properties. Also it is assumed that the interior of the system exhibits bulk properties. Remarkable agreement with experimental results for vapor phase homogeneous nucleation has been obtained with this liquid drop model. However, a variety of properties cannot be explained from a continuum model, especially in the limit of very small clusters. Atomistic models for microclusters can be divided into static and dynamic models. Calculations in the static mode usually treat relaxations by introducing variations in the atomic configuration until a minimum potential energy situation is achieved. The imposed variation can be a linear scaling of the cluster as a whole [5], independent variation of the radius of the individual neighbour shells [6], or the cluster may be allowed to relax freely in a quasidynamic mode [7]. Having thus established the zero-temperature atomic configuration, the thermodynamic properties at finite temperatures can be deduced within the framework of the harmonic approximation [8]. The inherent limitations of the harmonic approximation, such as its restriction to a single configuration [9] and the neglect of anharmonic effects, can be overcome only by applying more elaborate methods. Two such methods have been used; the Monte Carlo method [10] and the molecular dynamics method [11-15].

The present paper reports results of molecular dynamics studies of two- and three-dimensional microclusters with Lennard-Jones interactions. The aim

of this study was to illuminate the characteristics of the melting transition in finite systems.

**2. Method and model.** — The standard molecular dynamics technique [16-18] was used to simulate the thermodynamic and structural properties of microclusters. The interatomic interaction was represented by a truncated Lennard-Jones pair potential. The truncation distance,  $r_{\text{trc}}$ , was chosen corresponding to a 54 neighbour-atom interaction. Two 2-dimensional microclusters, containing 55 and 105 atoms, initially arranged in a hexagonal lattice configuration, and three 3-dimensional microclusters, containing 55, 135, and 429 atoms, initially arranged in an FCC lattice configuration, were considered. The simulations were performed on stationary clusters i. e. no net translation or rotation of the clusters was allowed. The boundary conditions, schematically shown in figure 1, were constructed to reinsert escaping atoms

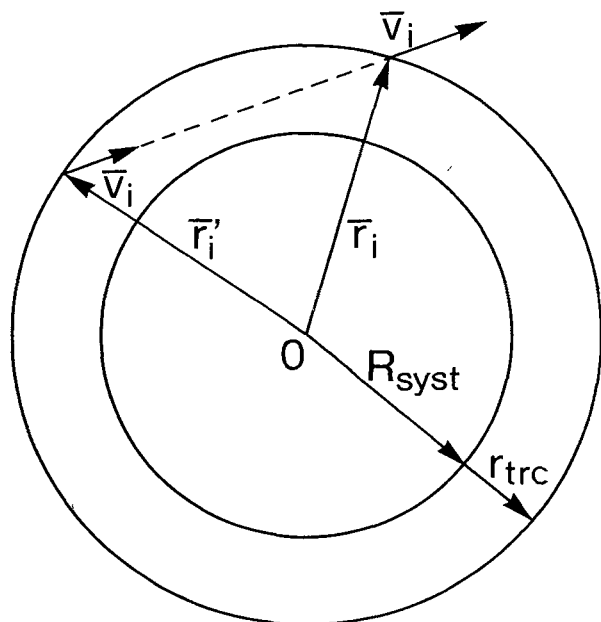


FIG. 1. — Boundary conditions for the finite systems. Escaping atoms (position  $\bar{r}_i$  and velocity  $\bar{v}_i$ ) are reinserted (position  $\bar{r}_i'$  and velocity  $\bar{v}_i'$ ) with conservation of linear and angular momenta.  $R_{\text{syst}}$  and  $r_{\text{trc}}$  are the radius of the relaxed crystal and the truncation distance applied to the interatomic potential.

in accord with the stationarity requirement, from escape position  $\bar{r}_i$  to entrance position  $\bar{r}_i'$ . The boundary condition implies a definition of an  $N$ -atom cluster configuration as one for which all  $N$  atoms are found within the distance  $R_{\text{syst}} + r_{\text{trc}}$  from the cluster centre of gravity,  $R_{\text{syst}}$  being the radius of the perfect  $N$ -atom cluster.

The properties of the different microclusters were simulated according to the following procedure. For each cluster a number of different thermodynamic states were realized by successive addition of small amounts of kinetic energy to the cluster starting out from a randomly distorted version of the initially

perfect atomic configuration. Each of the thermodynamic states thus obtained, characterized by a specific value of the cluster total energy, were subsequently simulated for a time period long enough to extract the thermodynamic and structural properties of the cluster at this specific value of the total energy. For details of the calculation of these properties see ref. [12] and [15] for the two- and three-dimensional systems respectively. The calculations were performed in units of  $\epsilon$ ,  $r_0$ ,  $m$ , and  $k_B$ , representing the depth and position of the minimum of the Lennard-Jones potential, the atomic mass, and Boltzmann's constant, respectively, and the results will be given in these units.

**3. The atomic structure of microclusters.** — When the model interatomic potential has been chosen, the structure of the bulk model system is fixed as well, thus for the Lennard-Jones potential the hexagonal lattice in two-dimensions, and the face centered cubic lattice in three-dimensions are the stable packing types of the systems. When the systems are of a finite extent, however, this statement no longer holds as can be anticipated from the following qualitative model for microclusters. The microcluster may be envisaged as consisting of two regions, a surface region and a core region. The surface region is characterised by atoms that are deprived of some of their neighbouring atoms, thus at the very surface approximately half the neighbour atoms are missing. Entering deeper into the microcluster this deficiency gradually disappears and at a depth corresponding to the effective range of the interatomic potential the effect of the free surface will be small. This marks the junction from the surface to the core region of the cluster. The interior core region having surroundings comparable to the bulk situation will tend to attain the bulk structure, and for sufficiently large clusters the surface region will have to adjust itself to this structure. For clusters so small that the ratio of surface atoms to core atoms becomes unity or more ( $N \leq 2000$  atoms in three dimensions), this overriding effect cannot persist and the possibility for different packing types in this size range will exist.

By applying the molecular dynamics method to the study of microclusters the existence of more exotic packing types can be revealed since this method in principle explores all accessible regions of the cluster phase space. Also this method offers a means of studying non-equilibrium situations. The detailed atomic mechanisms involved in transformations in the solid state as well as in the melting transition can be studied and transport properties of the clusters can be evaluated.

For the two-dimensional systems the following structural features were observed. The hexagonal packing persisted in the solid phase, and as the melting transition was approached, the surface became increasingly more diffuse and irregular, allowing sur-

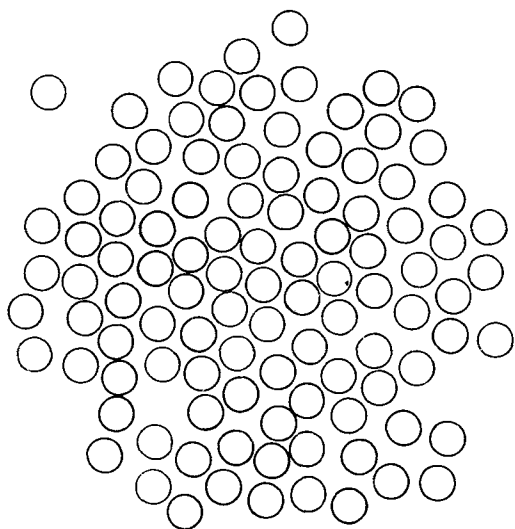


FIG. 2. — The two-dimensional 105-atom system shown at the onset of melting. A dislocation has been formed in the surface region.

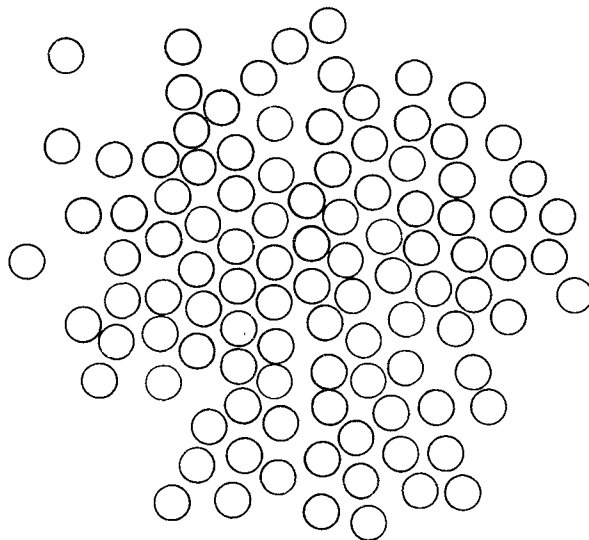


FIG. 3. — The two-dimensional 105-atom system shown at an advanced stage of the melting process. The surface has become very diffuse and several dislocations are observed in the surface region.

face diffusion to take place well below the melting temperature. Figures 2 and 3 show the 105-atom cluster at the onset of melting and at a more advanced state of the melting process. It appears that the surface becomes extremely diffuse during melting and that the melting process is associated with the formation of dislocations [19].

Evaporation was observed to appear frequently during the latter stages of melting especially for the smallest system. This circumstance, taken together with the reinsertion of escaping atoms, resulted in a

pressure increase for the high energy states. It was not possible, therefore, to study thoroughly the liquid state of the two-dimensional systems under zero pressure condition, and transitions from heated solid states to supercooled liquid states were not observed in these systems.

For the three-dimensional microcrystals the most stable packing types were found to be icosahedral for the 55-atom cluster and face centered cubic for the 135- and 429-atom clusters. If set up in an FCC configuration, the 55-atom cluster very rapidly transformed into the icosahedral configuration, provided the temperature was not too low. At temperatures below  $0.015 [e/k_B]$  the FCC configuration persisted through simulations of 20,000 timesteps, corresponding approximately to 150 atomic vibrational periods. The structure of the clusters is shown in figures 4-6, showing the pair distribution function for the three clusters, evaluated with the central atom as datum point at four different values of the cluster energy. From bottom to top the curves represent: *A*) a solid configuration at a low temperature, *B*) a solid at a higher temperature, *C*) a supercooled liquid at the same temperature as *B*), and *D*) a liquid configuration above the melting temperature. Apart from reflecting the icosahedral and FCC packings in the solid state (the positions and numbers of atoms in the neighbor shells of the FCC packing are indicated below in figures 5 and 6) the distribution functions also reveal the diffuse character of the surface at higher temperatures. In this respect the icosahedron constitutes an exception as it is characterised by a very dense and rather well defined surface even at temperatures close to the melting region. For the three-dimensional systems no evaporation of significance was observed, even at the highest energies simulated. Thus the zero

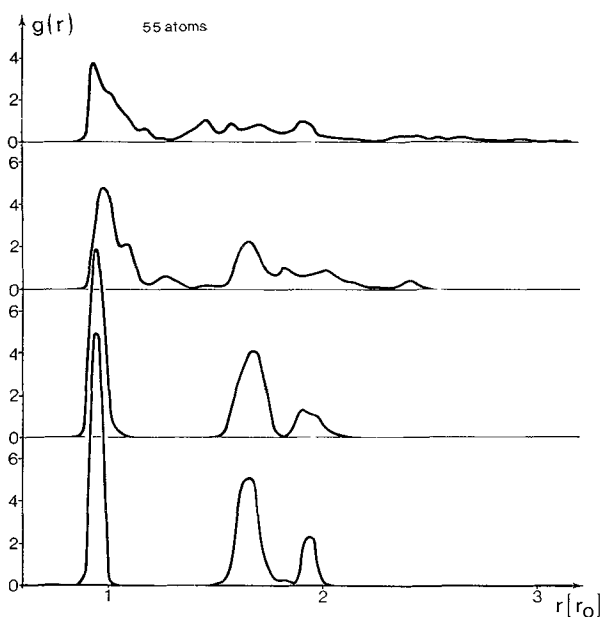


FIG. 4. — Pair distribution functions of the three-dimensional 55-atom cluster calculated with the central atom as datum point. The sequence from bottom to top corresponds to the sequence A, B, C, and D of figure 11.

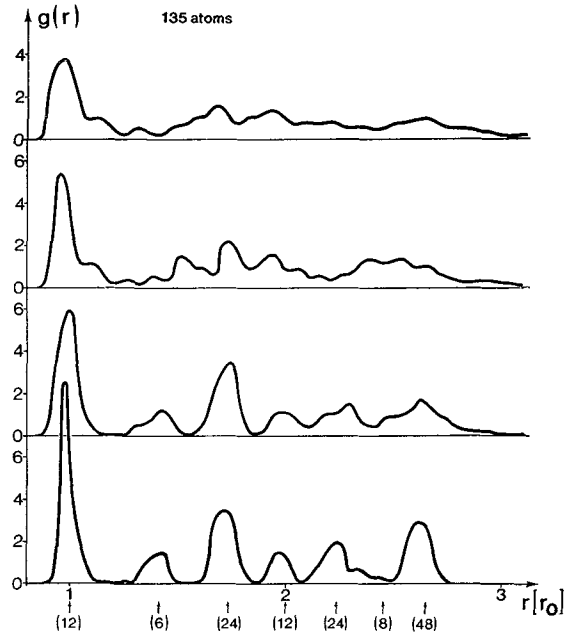


FIG. 5. — Pair distribution functions of the 135-atom cluster calculated with the central atom as datum point. The sequence from bottom to top corresponds to the sequence A, B, C, and D of figure 12. The arrows on the abscissa give the positions of the neighbour shells in the FCC system. The corresponding figures give the number of neighbours contained in each shell.

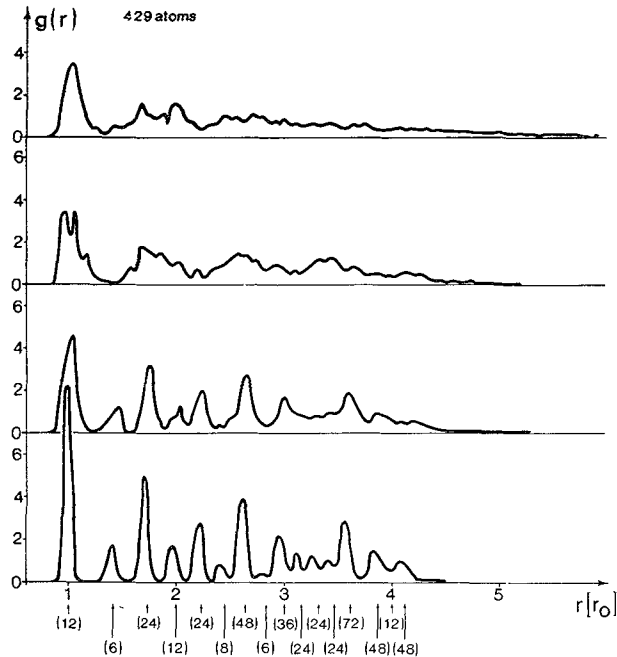


FIG. 6. — Pair distribution functions of the 429-atom cluster calculated with the central atom as datum point. The sequence from bottom to top corresponds to the sequence A, B, C, and D of figure 13. The arrows on the abscissa give the positions of the neighbour shells in the FCC system. The corresponding figures give the number of neighbours contained in each shell.

pressure condition could be maintained also in the liquid state. The transition from the solid to the liquid configuration was found to be of a spontaneous character. For a range of total energies each of the

clusters performed very rapid transitions to liquid-like configurations. The time spent in the solid configuration before the transition took place was found to decrease for increasing total energy of the cluster. A similar phenomenon, indicating that coexistence of the solid and liquid phases in small systems is not possible, has earlier been observed on systems with periodic boundary conditions [20]. For the clusters it was not possible to realize and maintain configurations representing intermediate states between the heated solid and the liquid configurations.

4. The thermodynamic properties of microclusters. —

The thermodynamic properties of the two-dimensional microclusters are shown in figures 7-10. The caloric equation of state, obtained by calculating the mean temperature at different values of the total energy, is plotted in figures 7 and 8. The zero temperature

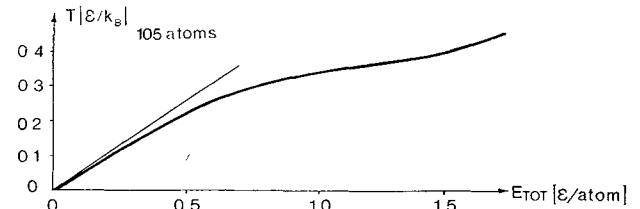


FIG. 7. — The caloric equation of state of the two-dimensional 55-atom cluster. The straight line indicates equipartition of energy.

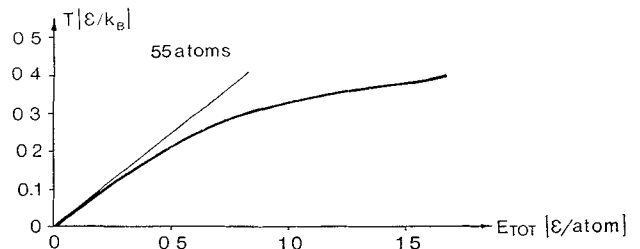


FIG. 8. — The caloric equation of state of the two-dimensional 105-atom cluster.

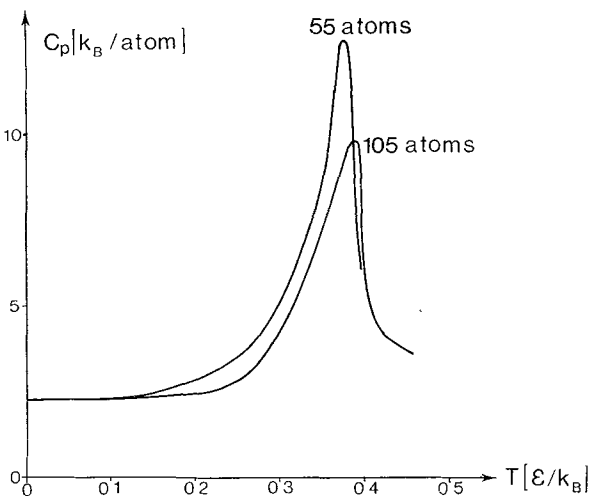


FIG. 9. — Specific heat curves for two-dimensional microclusters containing the number of atoms indicated.

potential energies of the relaxed microcrystals were  $-2.77$  and  $-2.93$  [ $\epsilon/\text{atom}$ ] for the 55- and 105-atom clusters respectively. These values were used as origin in the subsequent energy calculations. The straight lines on these plots represent equipartition of energy as it would be observed in a harmonic system. The appearance of anharmonic effects even at low temperatures is clearly seen. By graphic differentiation the specific heat curves of figure 9 are obtained. Simulation of a two-dimensional system with periodic boundary conditions [19] shows that the melting point of the *infinite* system is close to  $0.47$  [ $\epsilon/k_B$ ]. Figure 9 thus shows that the finite systems exhibit a melting point depression and that the transition is smoothed out over a fairly broad temperature range. The apparently larger latent heat of melting of the smallest system is probably due to the larger evaporation observed for this system, i. e. a comparably larger part of the latent heat of evaporation may be included for the small system. By integration the entropy shown in figure 10 is obtained, again the smeared out nature of the transition is displayed.

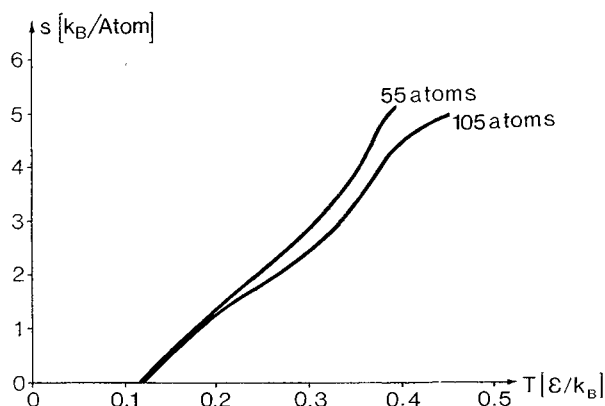


FIG. 10. — Entropy variation with temperature for the two-dimensional clusters.

By inspection of figures 11-20, showing the results for the three-dimensional systems, the same trend in the thermodynamic behaviour as observed for the two-dimensional systems is found. Figures 11-13 show

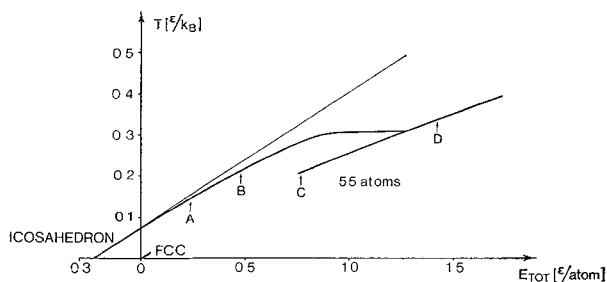


FIG. 11. — The caloric equation of state for the three-dimensional 55-atom system. The straight line represents equipartition of energy. The low-temperature properties of the metastable FCC system are also shown.

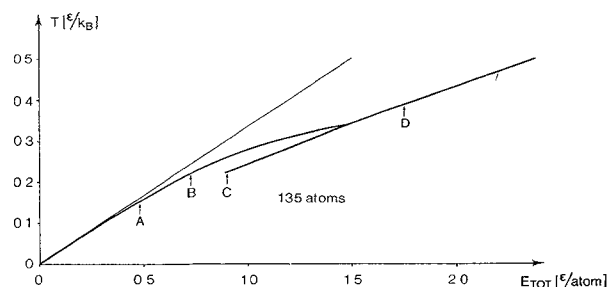


FIG. 12. — The caloric equation of state for the three-dimensional 135-atom system.

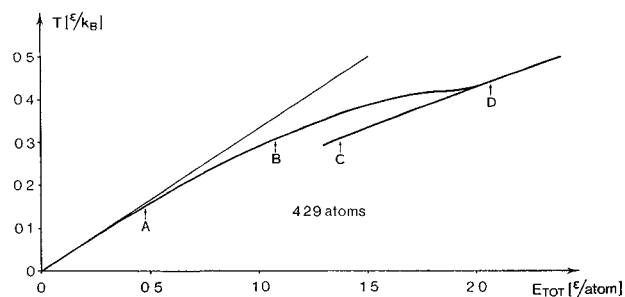


FIG. 13. — The caloric equation of state for the three-dimensional 429-atom system.

the caloric equation of state plotted with the origin of the energy-axes located at the potential energy at zero temperature of the relaxed FCC structures. The zero temperature potential energies  $\phi_0$  for the various clusters are listed in table I.

TABLE I

*Zero temperature properties and melting parameters for the microcrystals compared with the results for the infinite system. The melting temperature  $T_M$ , latent heat of melting  $L_M$ , and entropy of melting  $S_M$  are listed. The entropy obtained from thermodynamic considerations as well as the entropy calculated from the observed frequency spectra are shown. The melting parameters for the infinite system are average values of the experimental data for argon, krypton, and xenon [22].*

	$\phi_0$ [ $\epsilon/\text{atom}$ ]	$R_{\text{sys}}$ [ $r_0$ ]	$T_M$ [ $\epsilon/k_B$ ]	$L_M$ [ $\epsilon/\text{atom}$ ]	$S_M^{\text{th}}$ [ $k_B/\text{atom}$ ]	$S_M^{\text{vib}}$ [ $k_B/\text{atom}$ ]
55 Ico.	- 4.992	1.908	0.31	0.36	1.15	0.80
55 FCC	- 4.765	1.971	—	—	—	—
135 FCC	- 5.543	2.598	0.33	0.13	0.40	0.30
429 FCC	- 6.243	4.035	0.42	0.27	0.65	0.48
$\infty$ FCC	- 7.880	—	0.69	1.67	1.71	—

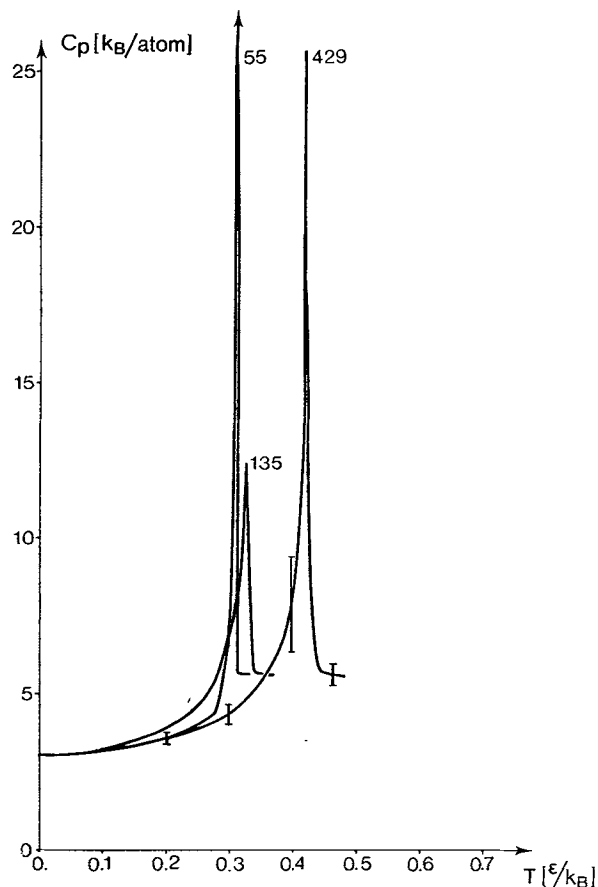


FIG. 14. — Specific heat curves for three-dimensional clusters containing the number of atoms indicated. The actual height of the 55-system peak is uncertain.

The melting point of the infinite three-dimensional Lennard-Jones system is close to 0.7. The specific heat curves of figure 14 thus show a pronounced and increasing melting point depression for decreasing microcrystal size. With respect to the tendencies in latent heat of melting and premelting behaviour the 55-atom icosahedron again constitutes an exception. The comparatively high melting temperature and relative sharpness of the transition as well as the suppression of premelting for this system may be due to the compact surface and also this special atomic packing type may oppose the formation of dislocations. The lower potential energy of the icosahedron gives rise to the large latent heat of melting  $L_M$  that characterises this system.

The frequency spectra of the three-dimensional systems measured in the states A, B, C, and D of the caloric equations of state are shown in figures 15-17. The spectra are calculated as the Fourier transform of the velocity auto-correlation functions as described by Dickey and Paskin [21]. From bottom to top the four spectra correspond to the sequence A, B, C, and D. In broad features the frequency distributions in the low temperature solid state are in agreement with those observed by Dickey and Paskin [11] for small particles. Remnants of the longitudinal bulk modes

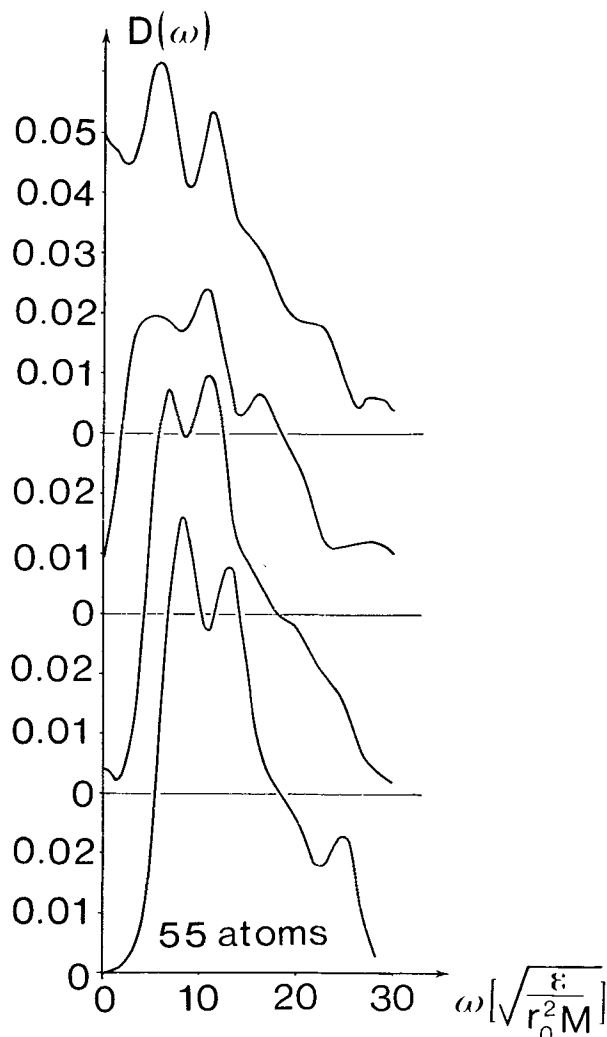


FIG. 15. — Frequency spectra of the 55-atom cluster. The distributions are calculated at the temperatures 0.148, 0.217, 0.211, and 0.341 going from bottom to top, corresponding respectively to the states labelled A, B, C, and D in figure 11.

that appear in the high-frequency end of the spectrum are seen to fade out with decreasing crystal size, whereas the peak located at about  $\omega = 9$  becomes more dominant. Dickey and Paskin identified this peak as a surface mode with amplitude normal to the surface, while the shoulder located at about  $\omega = 5$  was linked to edge atoms. This edge mode is seen to grow with decreasing crystal size, because of the larger surface to volume ratio, while for the icosahedral system it disappears completely apparently because of the compact surface composition of this structure. The diffusive properties of the clusters are revealed by the extreme low- $\omega$  part of the distributions. Diffusive modes of motion will contribute to this part of the frequency spectrum as it is seen in the liquid states C and D. Even in the high temperature solid states B, the diffuse surface results in a detectable diffusion.

The entropy of the microclusters were calculated by integration from the specific heat curves starting

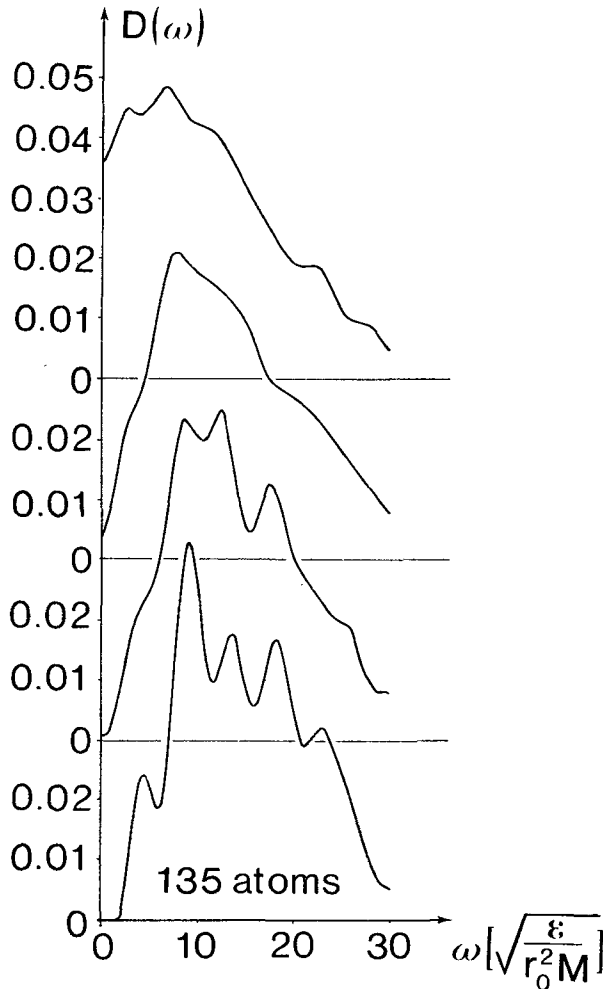


FIG. 16. — Frequency spectra of the 135-atom cluster. The temperatures are 0.152, 0.220, 0.222, and 0.387 from bottom to top, corresponding to A, B, C, and D respectively of figure 12.

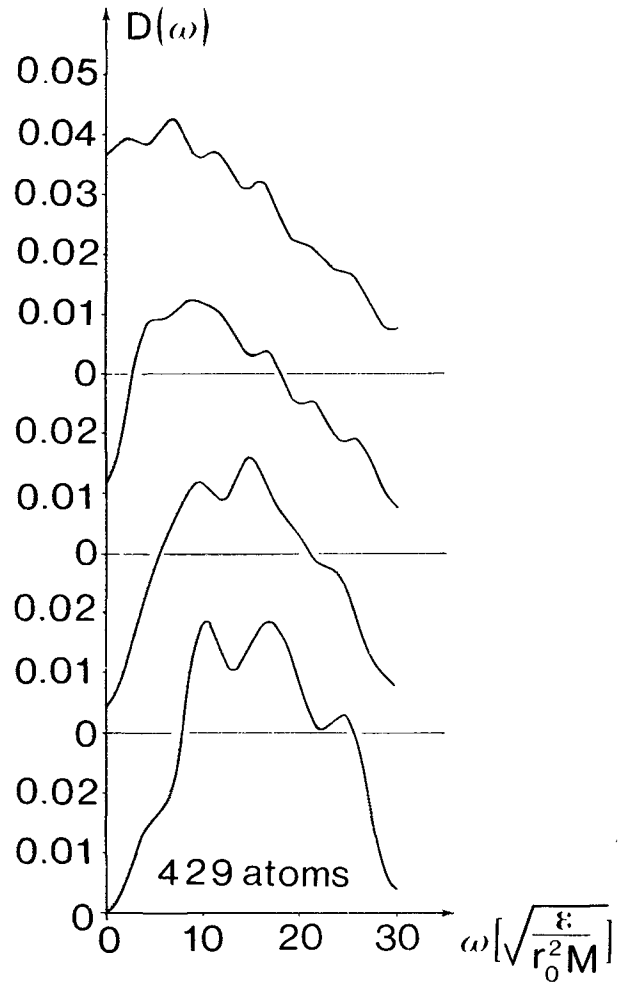


FIG. 17. — Frequency spectra of the 429-atom cluster. The temperatures are 0.153, 0.306, 0.309, and 0.442 from bottom to top, corresponding to A, B, C, and D respectively of figure 13.

out from  $T = 0.2$  [ $\epsilon/k_B$ ]. The result is shown as the lower curves of figures 18-20. Also shown (upper curves) is the result of the frequency histogram integration

$$s(T) = \frac{k_B}{N} \sum_i D(\omega_i) \left( 1 - \ln \frac{\hbar \omega_i}{k_B T} \right) \Delta \omega_i$$

which is a harmonic approximation formula valid in the classical limit of  $k_B T > \hbar \omega$ . Considering the origin of the entropy formula the agreement is remarkable, the deviation in entropy differences being of the order of 20 % even in the liquid temperature range.

**5. Conclusion.** — The molecular dynamics simulations of two-dimensional microclusters show that the melting transition is associated with the formation of dislocations. A melting point depression relative to the infinite system is observed, the depression being larger the smaller the system. Premelting is observed and the transition is found to take place over a broad temperature range in which evaporation is also active.

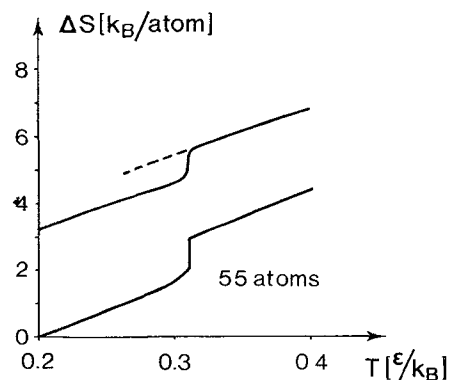


FIG. 18. — Entropy variation with temperature for the three-dimensional 55-atom system. The upper curve is calculated from the vibrational spectrum, the lower one is derived from the caloric equation of state. The dotted branch represents a supercooled liquid state.

This strong evaporation tendency was not observed for the three-dimensional systems for which well defined liquid configurations could be realized. The trends in thermodynamic properties for the three-

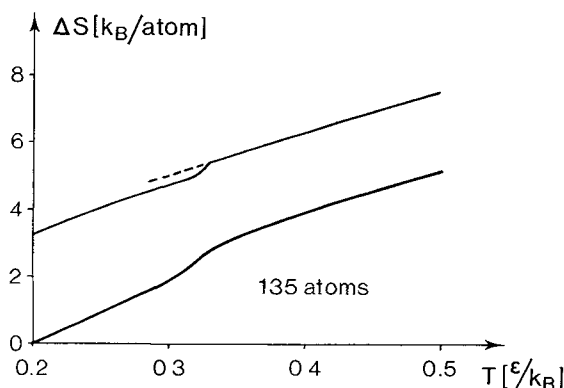


FIG. 19. — Entropy variation with temperature for the 135-atom system. The upper curve is calculated from the vibrational spectrum, the lower one is derived from the caloric equation of state. The dotted branch represents a super-cooled liquid state.

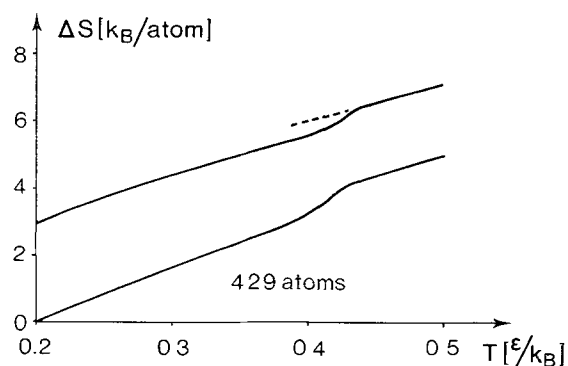


FIG. 20. — Entropy variation with temperature for the 429-atom system. The upper curve is calculated from the vibrational spectrum, the lower one is derived from the caloric equation of state. The dotted branch represents a super-cooled liquid state.

dimensional systems were increasing melting point depression and premelting and decreasing latent heat of melting for decreasing cluster size. The 55-atom icosahedron was observed to behave atypically because of its lower potential energy and denser surface structure. The melting process in the three-dimensional microcrystals was found to be of an abrupt

character rather than a gradual process starting at the surface.

**6. Acknowledgments.** — One of the authors (WDK) acknowledges financial support from the Danish Technical Science Research Council (Statens Teknisk-Videnskabelige Forskningsråd).

#### References

- [1] MORRISON, J. A., DRAIN, I. E. and DUGDALE, J. S., *Can. J. Chem.* **30** (1952) 890.
- [2] CURZON, A. E. and CHLEBEK, H. G., *J. Phys. F: Metal Phys.* **3** (1973) 1.
- [3] FARGES, J., RAOULT, B. and TORCHET, G., *J. Chem. Phys.* **59** (1973) 3454.
- [4] DUNNING, W. J., *Nucleation*, Ed. by A. C. Zettlemeyer (Dekker) 1969.
- [5] ALLPRESS, J. G. and SANDERS, J. V., *Australian J. Phys.* **23** (1970) 23.
- [6] BURTON, J. J., *J. Chem. Phys.* **52** (1970) 345.
- [7] HOARE, M. R. and PAL, P., *J. Cryst. Growth* **17** (1972) 77.
- [8] HILL, T. L., *An Introduction to Statistical Mechanics* (Addison Wesley) 1960, Chap. 9.
- [9] MCGINTY, D. J., *Chem. Phys. Lett.* **13** (1972) 525.
- [10] LEE, J. K., BARKER, J. A. and ABRAHAM, F. F., *J. Chem. Phys.* **58** (1973) 3166.
- [11] DICKEY, J. M. and PASKIN, A., *Phys. Rev. B* **1** (1970) 851.
- [12] COTTERILL, R. M. J., DAMGAARD KRISTENSEN, W., MARTIN, J. W., PEDERSEN, L. B. and JENSEN, E. J., *Computer Phys. Comm.* **5** (1973) 28.
- [13] MCGINTY, D. J., *J. Chem. Phys.* **58** (1973) 4733.
- [14] BRIANT, C. L. and BURTON, J. J., *Nature Phys. Sci.* **243** (1973) 100.
- [15] DAMGAARD KRISTENSEN, W., JENSEN, E. J. and COTTERILL, R. M. J., *J. Chem. Phys.* **60** (1974) 4161.
- [16] ALDER, B. J. and WAINWRIGHT, T., *J. Chem. Phys.* **31** (1959) 459.
- [17] GIBSON, J. B., GOLAND, A. N., MILGRAM, M. and VINEYARD, G. H., *Phys. Rev.* **120** (1960) 1229.
- [18] RAHMAN, A., *Phys. Rev.* **136** (1964) A 405.
- [19] COTTERILL, R. M. J. and PEDERSEN, L. B., *Solid State Commun.* **10** (1972) 439.
- [20] ALDER, B. J. and WAINWRIGHT, T. E., *Phys. Rev.* **127** (1962) 359.
- [21] DICKEY, J. M. and PASKIN, A., *Phys. Rev.* **188** (1969) 1407.
- [22] POLLACK, G. L., *Rev. Mod. Phys.* **36** (1964) 748.